

Calcium-based coordination polymers from a solvothermal synthesis of HKUST-1 in 3D printed autoclaves

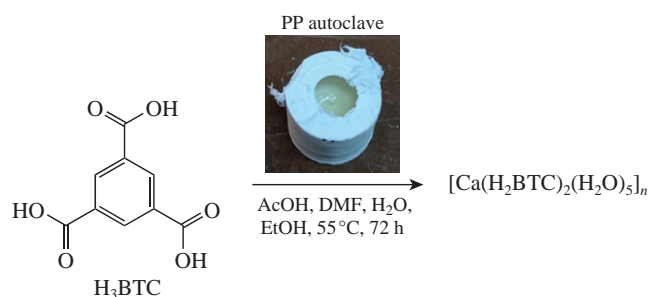
Petr V. Primakov,^{a,b} Gleb L. Denisov,^a Valentin V. Novikov,^a Olga L. Lependina,^a
Alexander A. Korlyukov^a and Yulia V. Nelyubina^{*a}

^a A. N. Nesmeyanov Institute of Organoelement Compounds, Russian Academy of Sciences, 119991 Moscow, Russian Federation. E-mail: unelya@ineos.ac.ru

^b D. I. Mendeleev University of Chemical Technology of Russia, 125047 Moscow, Russian Federation

DOI: 10.1016/j.mencom.2022.01.034

A mixed-metal 1D coordination polymer $[\text{CaCu}(\text{H}_3\text{BTC})_2(\text{H}_2\text{O})_8]_n$ (where H_3BTC – benzene-1,3,5-tricarboxylic acid) was obtained in a solvothermal synthesis of a well-known copper-containing metal–organic framework $[\text{Cu}_3(\text{BTC})_2(\text{H}_2\text{O})_3]_n$ (HKUST-1) in autoclaves 3D-printed from commercial polypropylene. This material was a source of calcium ions, apparently, leaking from a colorant (calcium carbonate) promoted by glacial acetic acid as a modulator used to produce large single crystals of HKUST-1. This finding was confirmed by elemental analysis and a model experiment that resulted in a new calcium-based 1D coordination polymer $[\text{Ca}(\text{H}_2\text{BTC})_2(\text{H}_2\text{O})_5]_n$ under the same solvothermal conditions with no copper or calcium salts put into a 3D-printed autoclave.



Keywords: 3D printing, 3D printed reactionware, autoclave, crystal structure, metal–organic coordination polymer, polypropylene, solvothermal synthesis, X-ray diffraction.

Coordination polymers (CPs) and metal–organic frameworks (MOFs)¹ are a unique class of crystalline materials built from metal ions or their clusters and organic ligands² that produce a periodic n -dimensional structure, $n = 1–3$. Featuring diverse and highly tunable properties,³ they found use as proton-conducting membranes,⁴ sensors^{5,6} and catalysts for various chemical reactions,^{7,8} including processes in the pores,⁹ in gas separation¹⁰ and storage,¹¹ targeted drug delivery,¹² and even structural biology.¹³ CPs and MOFs are typically obtained, among other synthetic approaches,¹⁴ under solvothermal conditions¹⁵ providing high-quality single crystals suitable for X-ray diffraction analysis, the method of choice for the identification of new crystalline materials, such as CPs and MOFs. In a solvothermal synthesis, organic and inorganic reagents are heated in a high-boiling polar solvent as a rule above its boiling point¹⁶ in commercial stainless steel autoclaves. These autoclaves are of a rather high cost and fixed (mostly, rather large) dimensions and have to be thoroughly cleaned after each use, thereby obstructing the search for new CPs and MOFs and optimization of the synthetic conditions through a high-throughput screening.¹⁷

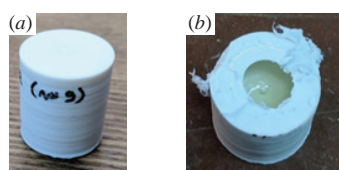
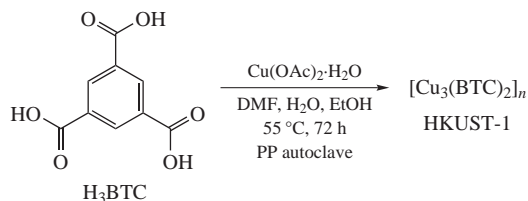


Figure 1 An autoclave from polypropylene (a) before and (b) after it has been opened.

As an alternative, disposable monolithic autoclaves (Figure 1) 3D-printed from thermally and chemically stable polypropylene have recently emerged.^{18,19} 3D printing, a very popular and accessible tool for fabrication of 3D-objects with complex geometries by layer-by-layer extrusion of a molten polymer or photopolymerization of acrylic resins,²⁰ has entered many areas of chemical science, from the creation of inexpensive (or otherwise unavailable) scientific equipment^{21–24} and reaction vessels and flow devices,^{18,20,25–27} including autoclaves for the solvothermal synthesis of CPs and MOFs,^{18,19,28,29} to generation of chemically active 3D-objects.³⁰ Unlike traditional stainless steel autoclaves, the polypropylene ones are inexpensive and come with desired dimensions, shapes and other characteristics. They can also be assembled into arrays for parallel synthesis and crystallization under identical conditions.^{18,19} If combined with automated dosing systems,³¹ this may open new horizons for the high throughput screening of CPs, MOFs¹⁷ and other types of crystalline materials produced under solvothermal conditions.³²

In this work, 3D-printed polypropylene autoclaves (Figure S1, Online Supplementary Materials) have been tested in the solvothermal synthesis of a well-known MOF $[\text{Cu}_3(\text{BTC})_2(\text{H}_2\text{O})_3]_n$ (HKUST-1) **1** by using a modified procedure (Scheme 1) reported to produce large single crystals of HKUST-1 from copper(II) salt and trimesic acid (H_3BTC) in the presence of glacial acetic acid used as a modulator.³³

Heating of the resulting solution in a 3D-printed polypropylene autoclave (polypropylene had been purchased from top3Dshop, <https://top3dshop.ru/>) at 55 °C for 72 h unexpectedly produced a



Scheme 1 Synthetic pathway to HKUST-1.

mixture of cubic blue single crystals as a major product and needle-like light-green ones as a minor product. After their careful examination by XRD,[†] the former appeared to be the expected HKUST-1,³⁷ while the latter represented a new mixed-metal 1D CP of the composition $[\text{CaCu}(\text{HBTC})_2(\text{H}_2\text{O})_8]_n$ **2** (Figure 2) similar to a reported cobalt(II) analogue $[\text{CaCo}(\text{HBTC})_2(\text{H}_2\text{O})_8]_n$ obtained from CaCl_2 , $\text{CoSO}_4 \cdot 7\text{H}_2\text{O}$ and trimesic acid.³⁸ As in the analogue, the asymmetric part of compound **2** contains one HBTC^{2-} dianion (instead of BTC^{3-} found in a similar copper(II)-based CP $[\text{Ca}_2\text{Cu}(\text{BTC})_2(\text{H}_2\text{O})_2]_n$),³⁹ copper(II) and calcium(II) cations that both occupy special positions (a four-fold roto-inversion axis and a two-fold rotation axis, respectively) and four metal-bound water molecules. A (pseudo)octahedral coordination of the Cu^{2+} ion is formed by two HBTC^{2-} dianions and four water molecules as well as additionally stabilized by an ‘intramolecular’ hydrogen bond $\text{O}(4\text{W})\text{---H}(4\text{WB})\cdots\text{O}(5)$ [$\text{O}\cdots\text{O}$ 2.997(4) Å, $\angle\text{O---H}\cdots\text{O}$ 135.27(18)°]. Ca^{2+} ion coordinates eight oxygen atoms from two HBTC^{2-} dianions, which act as a bridge between the two types of the metal ions, as well as four water molecules to produce a triangular dodecahedron (snub disphenoid) coordination environment as follows from the polyhedron type analysis⁴⁰ using the SHAPE2 software⁴¹ ($S = 1.998$).

In contrast to the known 3D CP $[\text{Ca}_2\text{Cu}(\text{BTC})_2(\text{H}_2\text{O})_2]_n$,³⁹ product **2** contains 1D polymer chains folded along the diagonal of *ac* crystallographic plane that are held together by numerous hydrogen bonds with $[\text{O}\cdots\text{O}$ 2.712(4)–2.880(4) Å, $\angle\text{O---H}\cdots\text{O}$ 160.4(2)–169.5(2)°] or between the coordinated water molecules $[\text{O}\cdots\text{O}$ 2.850(4)–3.370(4) Å, $\angle\text{O---H}\cdots\text{O}$ 159.1(2)–176.0(2)°] and between the HBTC^{2-} dianions. Combined with parallel displaced stacking interactions with an intercentroid distance of 3.4513(10) Å and an interplane angle of 2.34(16)° as well as shift distances of

[†] Single crystals of HKUST-1, **2** and **3** were collected from the polypropylene autoclaves after they cooled down to room temperature.

Crystal data for HKUST-1. $\text{C}_{18}\text{H}_{12}\text{Cu}_3\text{O}_{15}$ ($M = 658.90$), cubic, space group $Fm\bar{3}m$, at 120 K: $a = 26.3198(10)$ Å, $V = 18232.6(12)$ Å³, $Z = 16$, $d_{\text{calc}} = 0.906$ g cm⁻³, $F(000) = 5232$. Intensities of 52986 reflections were measured [$\lambda(\text{MoK}\alpha) = 0.71073$ Å, $\mu(\text{MoK}\alpha) = 14.25$ cm⁻¹, ω -scans, $2\theta < 56^\circ$], 1148 independent reflections ($R_{\text{int}} = 0.0484$) were used for the structure solution and refinement. Final R factors: $R_1 = 0.0281$ for 988 observed reflections with $I > 2\sigma(I)$, $wR_2 = 0.0890$ and GOF = 1.127 for all the independent reflections.

Crystal data for 2. $\text{C}_{18}\text{H}_{24}\text{CaCuO}_{20}$ ($M = 663.99$), monoclinic, space group $C2/c$, at 120 K: $a = 17.798(3)$, $b = 20.022(3)$ and $c = 6.5411(10)$ Å, $\beta = 96.309(3)^\circ$, $V = 2316.8(6)$ Å³, $Z = 4$, $d_{\text{calc}} = 1.904$ g cm⁻³, $F(000) = 1364$. Intensities of 12076 reflections were measured [$\lambda(\text{MoK}\alpha) = 0.71073$ Å, $\mu(\text{MoK}\alpha) = 12.68$ cm⁻¹, ω -scans, $2\theta < 54^\circ$], 2508 independent reflections ($R_{\text{int}} = 0.0766$) were used for the structure solution and refinement. Final R factors: $R_1 = 0.0477$ for 1969 observed reflections with $I > 2\sigma(I)$, $wR_2 = 0.1344$ and GOF = 1.030 for all the independent reflections.

Crystal data for 3. $\text{C}_{18}\text{H}_{20}\text{CaO}_{17}$ ($M = 548.42$), monoclinic, space group $P2_1/c$, at 120 K: $a = 13.3262(12)$, $b = 3.8494(4)$ and $c = 21.898(2)$ Å, $\beta = 101.562(3)^\circ$, $V = 1100.52(18)$ Å³, $Z = 2$, $d_{\text{calc}} = 1.655$ g cm⁻³, $F(000) = 568$. Intensities of 22217 reflections were measured [$\lambda(\text{MoK}\alpha) = 0.71073$ Å, $\mu(\text{MoK}\alpha) = 3.75$ cm⁻¹, ω -scans, $2\theta < 54^\circ$], 2384 independent reflections ($R_{\text{int}} = 0.1249$) were used for the structure solution and refinement. Final R factors: $R_1 = 0.0795$ for 1689 observed reflections with $I > 2\sigma(I)$, $wR_2 = 0.2225$ and GOF = 1.072 for all the independent reflections.

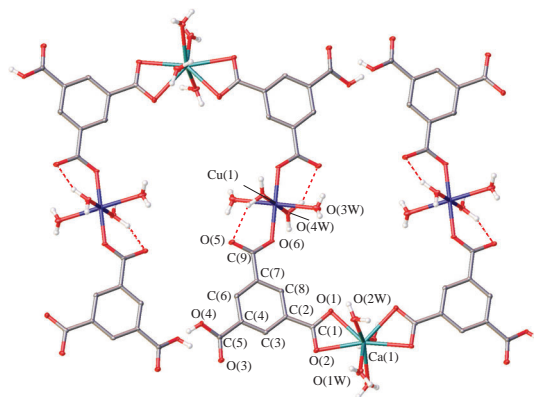


Figure 2 General view of **2** illustrating the formation of a 1D CP. Atoms are drawn as thermal ellipsoids at 30% probability level, hydrogen bonds are depicted by dashed lines. Selected bond lengths (Å): $\text{Ca}(1)\text{---O}(1)$ 2.468(3), $\text{Ca}(1)\text{---O}(2)$ 2.519(3), $\text{Ca}(1)\text{---O}(1\text{W})$ 2.381(3), $\text{Ca}(1)\text{---O}(2\text{W})$ 2.443(3), $\text{Cu}(1)\text{---O}(6)$ 1.988(2), $\text{Cu}(1)\text{---O}(3\text{W})$ 2.372(3) and $\text{Cu}(1)\text{---O}(4\text{W})$ 1.990(2).

1.036(5) and 1.117(5) Å, which assemble the benzene moieties of the adjacent chains into infinite stacks, they produce a dense 3D framework (Figure S2, Online Supplementary Materials), the volume of the largest spherical pore being 4.19 Å³.

Powder X-ray diffraction of the dried mixture of HKUST-1 and **2** showed it to be almost exclusively HKUST-1 with a contribution from compound **2** so small that it did not appear in the XRD pattern (Figure S3).

Among possible sources of calcium(II) ions in this mixedmetal 1D CP are the distilled water used as a solvent, which may contain (although highly unlikely) traces of calcium salts, or the material of the 3D-printed autoclave (although unheard of^{1–4}) that may contain calcium carbonate to give the white color to the naturally straw-colored polypropylene.^{18,19,28,29} In favor of the latter scenario, a report exists on CaCO_3 added to polypropylene for 3D-printing for the improvement of processability and the quality of printed items.⁴²

Our attempts to perform the synthesis under the same solvothermal conditions with no copper or calcium salts put into an otherwise identical reaction mixture in an autoclave 3D-printed from the same batch of the polypropylene (Scheme 2) repeatedly gave a few colorless needle-like crystals. According to XRD data, the product represented a new 1D CP $[\text{Ca}(\text{H}_2\text{BTC})_2(\text{H}_2\text{O})_5]_n$ **3** (Figure 3). In contrast to the mixed-metal 1D CP **2** and the known calcium-containing 2D⁴³ and 3D⁴⁴ CPs of the composition $[\text{Ca}_3(\text{BTC})_2(\text{H}_2\text{O})_{12}]_n$ as well as the 1D CP⁴⁵ $[\text{Ca}(\text{HBTC})\cdot 2\text{H}_2\text{O}]_n$ and the 3D CP $[\text{Ca}(\text{HBTC})(\text{H}_2\text{O})\cdot 2\text{H}_2\text{O}]_n$, one Ca^{2+} cation in compound **3** coordinates two H_2BTC^- anions as a bidentate and a monodentate ligands, respectively, as well as four water molecules that form a pentagonal bipyramid-like coordination environment as follows from the appropriate continuous shape measure⁴⁰

Data were obtained on a Bruker APEX2 DUO CCD diffractometer. Employing an OLEX2 software,³⁴ the structures were solved with a SHELXT structure solution program³⁵ using the intrinsic phasing mode and refined with an XL package³⁶ using the least squares minimization. Hydrogen atoms of the OH groups in the anions BTC^{3-} , HBTC^{2-} and H_2BTC^- as well as those of water molecules were found using the difference Fourier synthesis, while positions of other hydrogen atoms were calculated, after that they all were refined in the isotropic approximation within the riding model. For HKUST-1 severely disordered water molecules in the pores were treated as a diffuse contribution to the overall scattering with the solvent mask routine implemented in the OLEX2 software.³⁴

CCDC 2090916, 2090917 and 2090918 contain the supplementary crystallographic data for HKUST-1, **2** and **3**, respectively. These data can be obtained free of charge from The Cambridge Crystallographic Data Centre via <http://www.ccdc.cam.ac.uk>.



Scheme 2 Synthetic pathway to $[\text{Ca}(\text{H}_2\text{BTC})_2(\text{H}_2\text{O})_5]_n$

($S = 2.374$). The resulting 1D zigzag polymer chains, which run along the crystallographic axis c , are additionally stabilized by ‘intramolecular’ hydrogen bonds between the H_2BTC^- anions and the metal-bound water molecules [$\text{O}\cdots\text{O}$ 2.748(10) and 2.864(6) Å, $\angle\text{O}-\text{H}\cdots\text{O}$ 175.0(6) and 160.9(3)°] as well as weak parallel-displaced stacking interactions with an intercentroid distance of the benzene moieties of 3.8494(4) Å, an interplane angle of 0.0(3)° and shift distances of 1.221(6) and 1.117(5) Å.

The fifth water molecule occurs between these polymer chains and hold them together by hydrogen bonds with the H_2BTC^- anions [$\text{O}\cdots\text{O}$ 2.838(5) and 2.864(6) Å, $\angle\text{O}-\text{H}\cdots\text{O}$ 155.2(3) and 160.9(3)°] and a metal-bound water molecule [$\text{O}\cdots\text{O}$ 2.849(12) Å, $\angle\text{O}-\text{H}\cdots\text{O}$ 114.6(5)°]. Assisted by the hydrogen bonds between the H_2BTC^- anions [$\text{O}\cdots\text{O}$ 2.569(4) and 2.578(4) Å, $\angle\text{O}-\text{H}\cdots\text{O}$ 160.5(2) and 168.8(2)°], a dense 3D framework (Figure S4) with the largest spherical pore of 2.14 Å³ emerges in the crystal of compound **3**.

To gain insight into the composition of the fabricated autoclaves as a source of the calcium(II) ions in 1D CP $[\text{Ca}(\text{H}_2\text{BTC})_2(\text{H}_2\text{O})_5]_n$, we performed elemental analysis of a 19×19 mm square item 3D-printed from the same batch of polypropylene (see above). It appeared to contain 0.47% admixture of calcium and <0.1% of titanium as a component of TiO_2 , which represented another colorant for commercial polypropylene. The calcium leakage from polypropylene is, apparently, behind the formation of calcium-based 1D CPs $[\text{CaCu}(\text{H}_2\text{BTC})_2(\text{H}_2\text{O})_8]_n$ and $[\text{Ca}(\text{H}_2\text{BTC})_2(\text{H}_2\text{O})_5]_n$ promoted by glacial acetic acid that was used as a modulator in the solvothermal synthesis of HKUST-1, as no such effects have been observed for 3D-printed autoclaves by us^{28,29} or other authors^{18,19} in its absence.

To experimentally confirm this hypothesis, we repeated the synthesis of HKUST-1, this time in a closed glass vial, and obtained pure HKUST-1 as followed from the visual inspection of single crystals collected immediately after cooling the vial to room temperature. There were only cubic blue crystals of HKUST-1 with no evidence for the admixture of the mixed-metal 1D CP **2**. The results from powder X-ray diffraction that indicate the purity of the dried product (see Figure S5) may be inconclusive, given a very minor amount of **2** formed under the corresponding conditions (see above), however, the known data³³ supported our conclusion.

The formation of the new calcium-based 1D CPs **2** and **3** is the first demonstration of the chemical activity³⁰ of autoclaves 3D-printed from commercial polypropylene. Sometimes, it may

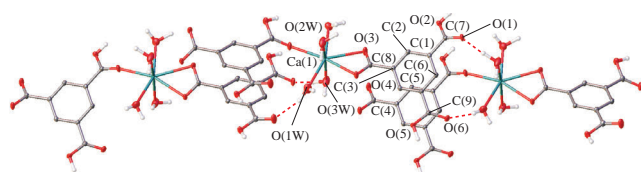


Figure 3 General view of **3** illustrating the formation of a 1D CP. Atoms are drawn as thermal ellipsoids at 30% probability level, hydrogen bonds are depicted by dashed lines. Non-coordinated water molecules (see the text) are omitted. Selected bond lengths (Å): Ca(1)–O(1) 2.402(3), Ca(1)–O(3) 2.595(3), Ca(1)–O(4) 2.487(3), Ca(1)–O(1W) 2.454(4), Ca(1)–O(2W) 2.46(4) and Ca(1)–O(3W) 2.272(8).

interfere with the synthesis of the target product by releasing calcium ions into the reaction mixture under the solvothermal conditions and thus producing unexpected CPs and MOFs similar to the breaking of these autoclaves upon heating when fabricated with non-optimal parameters of 3D-printing.²⁸ Even though a defect, it may result in crystalline products previously unheard of, thereby contributing to the discovery of new CPs and MOFs optimized for various applications of these versatile materials in science and technology.

This work was supported by the Russian Foundation for Basic Research (project no. 19-29-08032). Elemental analysis was performed using the equipment of Center for molecular composition studies of INEOS RAS with the financial support from Ministry of Science and Higher Education of the Russian Federation.

Online Supplementary Materials

Supplementary data associated with this article can be found in the online version at doi: 10.1016/j.mencom.2022.01.034.

References

- O. M. Yaghi and H. Li, *J. Am. Chem. Soc.*, 1995, **117**, 10401.
- O. M. Yaghi, M. O’Keeffe, N. W. Ockwig, H. K. Chae, M. Eddaoudi and J. Kim, *Nature*, 2003, **423**, 705.
- D. N. Dybtsev, A. A. Sopianik and V. P. Fedin, *Mendeleev Commun.*, 2017, **27**, 321.
- M. Yoon, K. Suh, S. Natarajan and K. Kim, *Angew. Chem., Int. Ed.*, 2013, **52**, 2688.
- L. M. Kustov, V. I. Isaeva, J. Přeč and K. K. Bisht, *Mendeleev Commun.*, 2019, **29**, 361.
- L. E. Kreno, K. Leong, O. K. Farha, M. Allendorf, R. P. Van Duyne and J. T. Hupp, *Chem. Rev.*, 2012, **112**, 1105.
- A. V. Stepanov, K. E. Mel’nik, V. I. Isaeva, G. I. Kapustin, V. V. Chernyshev and V. V. Veselovsky, *Mendeleev Commun.*, 2018, **28**, 88.
- J. Cui, M. Zhang, C. Wei, J. Zhu, X. Wang and X. Du, *Mendeleev Commun.*, 2020, **30**, 282.
- J. Lee, O. K. Farha, J. Roberts, K. A. Scheidt, S. T. Nguyen and J. T. Hupp, *Chem. Soc. Rev.*, 2009, **38**, 1450.
- Z. R. Herm, B. M. Wiers, J. A. Mason, J. M. van Baten, M. R. Hudson, P. Zajdel, C. M. Brown, N. Masciocchi, R. Krishna and J. R. Long, *Science*, 2013, **340**, 960.
- C. E. Wilmer, M. Leaf, C. Y. Lee, O. K. Farha, B. G. Hauser, J. T. Hupp and R. Q. Snurr, *Nat. Chem.*, 2012, **4**, 83.
- M. Giménez-Marqués, T. Hidalgo, C. Serre and P. Horcajada, *Coord. Chem. Rev.*, 2016, **307**, 342.
- Y. Inokuma, S. Yoshioka, J. Ariyoshi, T. Arai, Y. Hitora, K. Takada, S. Matsunaga, K. Rissanen and M. Fujita, *Nature*, 2013, **495**, 461.
- N. Stock and S. Biswas, *Chem. Rev.*, 2012, **112**, 933.
- Y. Zhao, K. Li and J. Li, *Z. Naturforsch., B: J. Chem. Sci.*, 2010, **65**, 976.
- X.-M. Chen and M.-L. Tong, *Acc. Chem. Res.*, 2007, **40**, 162.
- E. Biemmi, S. Christian, N. Stock and T. Bein, *Microporous Mesoporous Mater.*, 2009, **117**, 111.
- P. J. Kitson, R. J. Marshall, D. Long, R. S. Forgan and L. Cronin, *Angew. Chem., Int. Ed.*, 2014, **53**, 12723.
- C.-G. Lin, W. Zhou, X.-T. Xiong, W. Xuan, P. J. Kitson, D.-L. Long, W. Chen, Y.-F. Song and L. Cronin, *Angew. Chem., Int. Ed.*, 2018, **57**, 16716.
- E. G. Gordeev and V. P. Ananikov, *Russ. Chem. Rev.*, 2020, **89**, 1507.
- C. Zhang, B. Wijnen and J. M. Pearce, *J. Lab. Autom.*, 2016, **21**, 517.
- T. Baden, A. M. Chagas, G. Gage, T. Marzullo, L. L. Prieto-Godino and T. Euler, *PLoS Biol.*, 2015, **13**, e1002086.
- B. Berman, *Business Horizons*, 2012, **55**, 155.
- N. P. Macdonald, G. L. Bunton, A. Y. Park, M. C. Breadmore and N. L. Kilah, *Anal. Chem.*, 2017, **89**, 4405.
- P. J. Kitson, S. Glatzel, W. Chen, C.-G. Lin, Y.-F. Song and L. Cronin, *Nat. Protoc.*, 2016, **11**, 920.
- M. D. Symes, P. J. Kitson, J. Yan, C. J. Richmond, G. J. T. Cooper, R. W. Bowman, T. Vilbrandt and L. Cronin, *Nat. Chem.*, 2012, **4**, 349.
- E. G. Gordeev, E. S. Degtyareva and V. P. Ananikov, *Russ. Chem. Bull., Int. Ed.*, 2016, **65**, 1637 (*Izv. Akad. Nauk, Ser. Khim.*, 2016, 1637).
- G. L. Denisov, P. V. Primakov and Yu. V. Nelyubina, *Russ. J. Coord. Chem.*, 2021, **47**, 253 (*Koord. Khim.*, 2021, **47**, 218).

- 29 G. L. Denisov, P. V. Primakov, A. A. Korlyukov, V. V. Novikov and Yu. V. Nelyubina, *Russ. J. Coord. Chem.*, 2019, **45**, 836 (*Koord. Khim.*, 2019, **45**, 713).
- 30 M. R. Hartings and Z. Ahmed, *Nat. Rev. Chem.*, 2019, **3**, 305.
- 31 A. J. Florence, A. Johnston, P. Fernandes, N. Shankland and K. Shankland, *J. Appl. Crystallogr.*, 2006, **39**, 922.
- 32 G. Demazeau, *J. Mater. Sci.*, 2008, **43**, 2104.
- 33 T. M. Tovar, J. Zhao, W. T. Nunn, H. F. Barton, G. W. Peterson, G. N. Parsons and M. D. LeVan, *J. Am. Chem. Soc.*, 2016, **138**, 11449.
- 34 O. V. Dolomanov, L. J. Bourhis, R. J. Gildea, J. A. K. Howard and H. Puschmann, *J. Appl. Crystallogr.*, 2009, **42**, 339.
- 35 G. M. Sheldrick, *Acta Crystallogr., Sect. A: Found. Adv.*, 2015, **71**, 3.
- 36 G. M. Sheldrick, *Acta Crystallogr., Sect. A: Found. Crystallogr.*, 2008, **64**, 112.
- 37 M. Eddaoudi, J. Kim, N. Rosi, D. Vodak, J. Wachter, M. Keeffe and O. M. Yaghi, *Science*, 2002, **295**, 469.
- 38 G. Liang, Y. Liu, X. Zhang and Z. Wei, *Synth. React. Inorg., Met.-Org., Nano-Met. Chem.*, 2016, **46**, 251.
- 39 F. Zhang and B.-G. Zhang, *Acta Crystallogr., Sect. E: Crystallogr. Commun.*, 2017, **73**, 835.
- 40 S. Alvarez, *Chem. Rev.*, 2015, **115**, 13447.
- 41 M. Llunell, D. Casanova, J. Cirera, P. Alemany and S. Alvarez, *SHAPE, version 2.1*, Universitat de Barcelona, 2013.
- 42 E. B. Evoro, Yu. V. Perukhin, R. R. Bilalov and T. R. Deberdeev, *Vestn. Kazan Tekhnol. Univ.*, 2017, **20** (21), 56 (in Russian).
- 43 Y.-Y. Yang, Z.-Q. Huang, L. Szeto and W.-T. Wong, *Appl. Organomet. Chem.*, 2004, **18**, 97.
- 44 R. K. Vakiti, B. D. Garabato, N. P. Schieber, M. J. Rucks, Y. Cao, C. Webb, J. B. Maddox, A. Celestian, W.-P. Pan and B. Yan, *Cryst. Growth Des.*, 2012, **12**, 3937.
- 45 M. J. Platers, R. A. Howie and A. J. Roberts, *Chem. Commun.*, 1997, 893.

Received: 8th July 2021; Com. 21/6606